Surface Finish Control in Machining Processes using Haralick Descriptors and Neuronal Networks

E. Alegre*, R. Alaiz-Rodríguez, J. Barreiro, E. Fidalgo, and L. Fernández

Dept. of Electrical, Automatic and Systems Engineering.
University of León, 24071 León, Spain.
Phone: 0034 987 291989,
Fax: 0034 987 291970,
Email: enrique.alegre@unileon.es

Abstract. This paper presents a method to perform a surface finish control using a computer vision system. The goal pursued was to design an acceptance criterion for the control of surface roughness of steel parts, dividing them in those with low roughness acceptable class and those with high roughness defective class. We have used 143 images obtained from AISI 303 stainless steel machining. Images were described using three different methods texture local filters, the first four Haralick descriptors from the gray-level co-ocurrence matrix and a 20 features vector obtained from the first subband of a wavelet transform of the original image and also the gray-level original image. Classification was conducted using K-nn and Neuronal Networks. The best error rate - 4.0% - with k-nn was achieved using texture descriptors. With the neuronal network, an eight node hidden layer network using Haralick descriptors leads to the optimal configuration - 0.0% error rate -.

Key words: roughness control, textural descriptors, Gray Level Co-ocurrence Matrix, k-nn, neuronal network, classification

1 Introduction

Surface measurement has been an important topic in the research during the last decades. The reason is that it constitutes an important property of parts and products with high significance in their functionality. In many situations, it is required to qualify and quantify diverse aspects of the surfaces: geometry, topography, texture, roughness and defects [18]. When the quality control point of view is considered, the necessity of evaluate the surface roughness is obvious, since it represents an important requirement in many engineering applications [1, 2, 19].

The measurement of surface roughness started a few decades ago with the advent of tactile profilometers. These drag a stylus along a line segment and record the vertical deflection of the stylus as it moves over the surface, thus recording the height of the surface at the sampling points. Using this traditional technology, the surface finish can be estimated by means of some roughness parameters defined in international standards [6]. Development of these standards is basically oriented to tactile measuring devices that provide twodimensional records of part profile.

However, even though the stylus instrument is still considered to be the accepted standard for measurement of surface roughness, the method has several disadvantages [18, 15]: a) the stylus has to stay in permanent contact with the surface and is therefore easily damaged or soiled; b) the single profile line covers only a small part of the surface, possibly missing important areas; c) surface damage in some instances by the stylus force; d) low efficiency due to scanning. More disadvantages of stylus-based method can be found in [19].

These numerous disadvantages of contact methods have forced to surface measurement technologies to evolve significantly during last years [1] towards non-contact methods. A large research has been done in order to characterize 3D measurements of surface without contact at once. Among the common techniques are white-light interferometry, fringe projection, microscopy, speckle, light scattering and others.

Among these modern techniques, those based on computer vision can be remarked in terms of speed and accuracy. The advantages this technology provides are diverse. Whereas tactile techniques characterize a linear track over the part surface, computer vision techniques allow characterizing wide areas of the part surface providing more information [15, 3, 16, 11]. Also, computer vision techniques take measures faster, since images are captured in a very short time, and they can be in-machine implemented. In addition, the application of exhaustive validity checking to each part is also possible. This aspect would be very difficult to achieve with traditional tactile porfilometers, which are slow and delicate.

Continuous advances have been made in sensor technologies. Particularly, vision sensors have been greatly enhanced in capabilities and cost reduction. Additionally, advances in image processing technology provide more reliable conclusions than before.

In all, computer vision is a very interesting technology for industrial environment. The use of these systems for the monitoring of machining operations has proved [12, 4] an important reduction in the cycle time and the required resources. In particular, the modeling and prediction of surface roughness by computer vision have received a great deal of attention [2–6, 8–12, 15–17, 19].

As far as the traditional contact techniques are concerned, computer vision techniques use other parameters to measure the surface finish. In the view of this consideration, the current standards developed for tactile devices do not reflect the current state of technology. New procedures are necessary to correlate the results obtained with tactile instruments with those obtained using other devices, as those based on computer vision. In this context, two lines should be remarked: the study on the spatial domain and the study in the frequency domain. This work tackles the measurement of surface quality from the point of view of the spatial domain.

Tarng and Lee [9] and Lee et al. [13] analyze the use of artificial vision and image analysis to quantify the roughness in different turning operations. Methods based on image analysis capture an image of the surface and analyze its pixels to obtain a diffuse light pattern. Later on, roughness parameters are calculated by means of statistical descriptors. One of the most used parameters is the standard deviation of gray levels. Kumar et al. [8] focus on milling, turning and molding processes. They make zoom over original images to obtain the Ga parameter (the image gray level average), finding a high correlation amongst the Ga parameter and the surface roughness. Kiran et al. [7] used a measure called texture unit, calculated from the gray scale values of the image, in order to describe the local texture of a pixel. Al-Kindi et al. [3] proposed a method named intensitytopography compatibility (ITC), characterizing the image data by three components: lightning, reflectance and surface characteristics. They calculate the value of conventional roughness parameters combining statistical such as mean value and standard deviation. Ramana and Ramamoothy [14] proposed a method based on the gray-level difference matrix for texture analysis. Tasan et al. [17] proposed a method for the comparison of local heights from the image data using successive surface images. Lee et al. [12] developed a computer vision system that measures the roughness in turning processes automatically.

In this work we propose a new method that can be used as an acceptance criterion in a quality control process. We have classified the roughness of carbon steel parts into two classes without error using texture descriptors.

The rest of the paper is organized as follows: Sect. 2 describes the image acquisition process. A description of the features used is included in Sect 3 and the classification stage in Sect. 4. Finally, conclusions are summarized in Sect. 5.

2 Samples and Image Acquisition

2.1 Test Parts and Machining Characteristics

Test parts were made of AISI 303 X8CrNiS189 stainless steel. This material was chosen due to its common use in the small part mass-manufacturing industry. A MUPEM CNC multiturret parallel lathe ICIAR/1/42 model was used for the machining of parts.

Fig. 1 shows the test part used. Several part operations were carried out, all of them representative of massive precision machining. However, only the cylindrical shape was used for surface finish measurement. Cutting tools were coated carbide inserts from Sandvik. The machining parameters used for the tests were fixed at the following values: cutting speed 250 m/min, feed rate 0.27 mm/rev and cutting depth 2 mm, considered as reference values. A surface finish control was performed on a HOMMELWELKE class 1 perfilometer. It was evident that the evolution of surface finish Ra values was far worse when increasing the machining time.

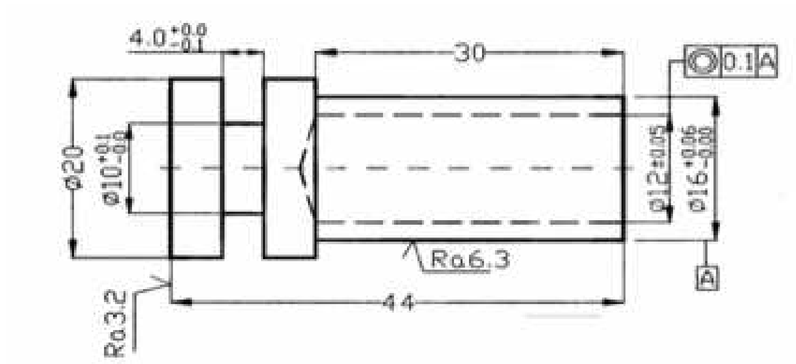

Fig. 1. Test parts used to measure the surface roughness.

2.2 Image Acquisition

Images of the parts were captured using a specific location fixture which had attached a camera and a diffuse lighting system (Fig. 2). The part was positioned onto a V shape bracket. The lighting system comprised a FOSTEC regulated light source DCR RIII. A NER SCDI-25-F0 diffuse illumination SCDI system was used to avoid shines. The system provided diffuse illumination in the camera axis.

The images were obtained using a Pulnix PE2015 B/W camera with 1/3 CCD. A Matrox Meteor II frame grabber card was used to digitize the images.

The optic assembly was composed of an OPTEM industrial zoom 70XL, with an extension tube of 1X and 0.5X/0,75X/1.5X/2.0X OPTEM lens. We used the maximum magnification of the system.

2.3 Experimental Image Set

Using such system, 143 images were captured (see Fig. 3) with the same z scale. Each of the images was labeled with its R_a roughness parameter, obtained using the median of three repeated R_a measuring. The roughness values were in the range 2.40 to 4.33 m.

Several experiments were carried out and the images were divided in two sets: the first class corresponds to low roughness (satisfactory) and the second class to high roughness (unacceptable). Images of both classes are shown in Fig. 3.

Three different cases were considered. In the first case, the first thirty images (ordered by R_a values) were separated from the last thirty and labeled as class 1 and class 2 respectively. In the second case, one class was composed by the first fifty images and the second one by the last fifty. In the third case, seventy of them were assigned to class 1 while the other seventy to class 2. Images of both classes will be included in train and test subgroups as explained in section 4.

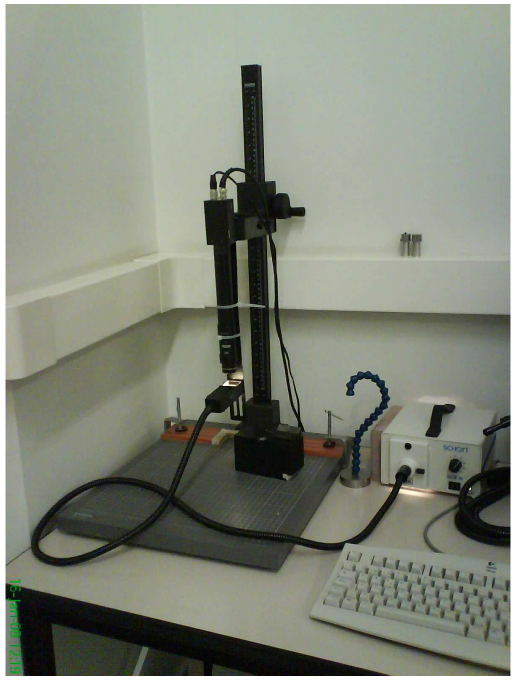

Fig. 2. Camera and lighting system used in the image acquisition.

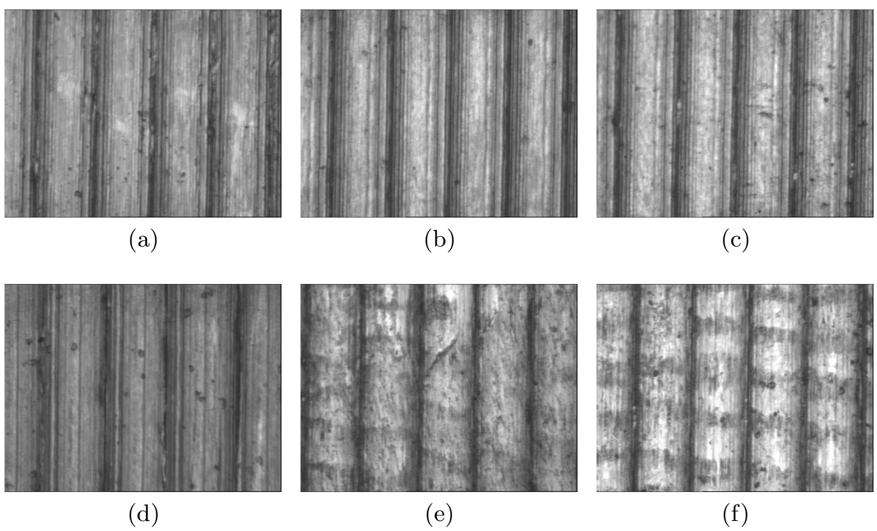

Fig. 3. Images of both classes 1 and 2. a, b and c with low roughness (R_a of 2.66, 2.77 and 2.82 μm respectively) and d, e and f with high roughness (R_a of 3.65, 4.03 and 4.03 μm)

3 Image processing and feature extraction methods

3.1 Image Preprocessing

A vertical Prewitt high pass filter was applied to the complete set of images in order to enhance contrast and make easier the description of roughness. Later on, three sets of descriptors were obtained for the original images and also for the filtered images. Fig. 4 a and b show two images with different Ra before filtering and c and d show the same images after filtering, all of them have the same z scale. Since a better performance was reached with filtered images, we only show values obtained when classifying with those images.

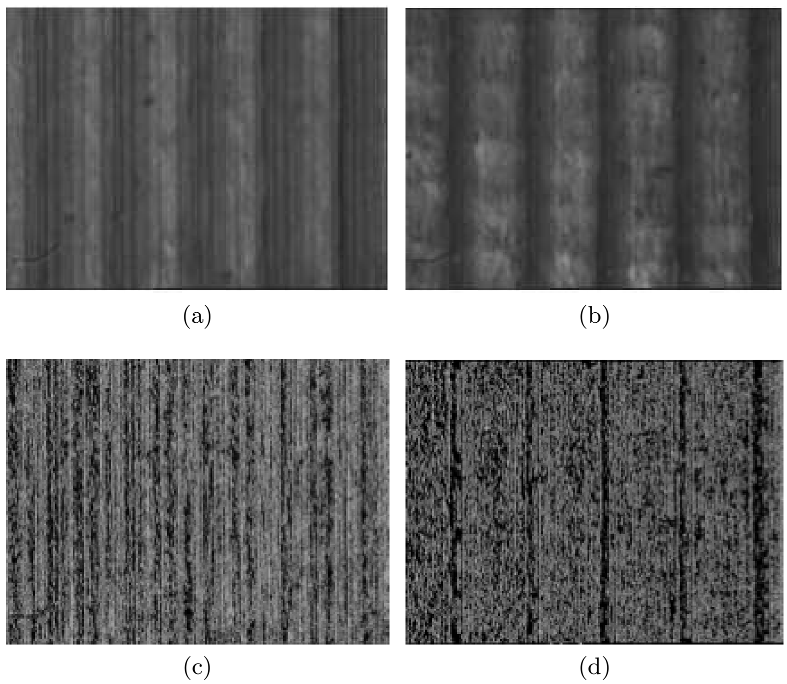

Fig. 4. a and b show original images with R_a of 2.47 μm -left- and 4.33 μm -right-. c and d show the same images after filtering.

3.2 Texture Descriptors

Three different feature vectors were obtained by computing some texture descriptors: three texture local features (entropy, range, and standard deviation), the four main Haralick features (Contrast, Correlation, Energy, Homogeneity) from the Gray Level Co-occurrence Matrix and twenty features from the Haralick descriptors applied over the original image and the first sub band of a Wavelet Transform of the original image.

4 Classification Methods

The former feature vectors were classified by means of k-nn using the random sampling validation method. This let us to compare the results of classification with those obtained by means of neural networks. The neural network used was a multilayer Perceptron (MLP) with sigmoidal transfer functions. The learning algorithm belongs to the group of backpropagation algorithms, in particular the Levenberg-Marquadt optimized version.

The feature vector values were normalized, in such a way that a translation and a scaling were applied to each random sampling extracted from the training set. The translation of the group of vectors was applied from its own centroid to the origin of the space in order to achieve a medium value of cero. The scaling was done dividing each vector by the medium energy of the group, calculated as the root mean square. This operation leads to a standard deviation value of one.

The optimum number of nodes in the hidden layer and the number of training cycles have been selected empirically. The validation method is a random sampling type. This method divided the available set of images in subgroups randomly, 70% for training and 30% for test. Performance is evaluated computing the mean error rate over ten runs. Also, the effect of data normalization over the classification error was analyzed.

4.1 k-Nearest Neighbors

The best results have been achieved with the texture local features descriptors.

The lower error is 4.0% for the case of fifty images by class. The error increases up to 10% and 9% when using thirty and seventy images respectively and the error distribution is fairly uniform among the classes. Table 1 shows the minimum errors in each class for the three descriptors used in this work.

Images	Local Texture	GLCM Descriptors	Haralick and Wavelet
30	10.56	6.11	8.33
50	**4.00**	5.00	5.00
70	9.05	6.90	8.33

Table 1. Minimal errors in each case. First column with local filters, second columns with GLCM (GrayLevelCoocurrenceMatrix) and first four Haralick descriptors and third column with the 20 features vector using wavelet.

4.2 Neural Network

The error rates obtained with the neural network are similar, lower than 10% for several descriptors. The error rate was 0.0% with fifty images in each class and using the Haralick descriptors obtained over the Wavelet transform. Only the Haralick descriptors enhance their results when using the vertical Prewitt filtering, the rest of them achieve significant better results when the filter is not applied.

All descriptors were used for this test, and the results obtained from them are acceptable, in most of the cases with error rates below 10.0%.

	Local Texture				**GLCM Descriptors**				**Haralick Wavelet**			
	25	**100**	**200**	**1000**	**25**	**100**	**200**	**1000**	**25**	**100**	**200**	**1000**
2	11.11	10.42	*9.03*	*9.03*	7.64	*6.94*	10.42	11.11	3.47	*2.78*	3.47	3.47
4	*9.03*	*9.03*	15.28	18.06	8.33	10.42	*7.64*	*7.64*	3.47	5.56	*2.78*	5.56
6	10.42	11.11	*8.33*	9.03	11.11	9.03	*7.64*	8.33	6.94	*1.39*	*1.39*	2.78
8	9.03	*7.64*	9.72	8.33	9.03	9.72	9.03	*7.64*	9.03	***0.69***	2.78	2.78
10	12.5	9.03	*6.25*	6.94	11.81	*8.33*	*8.33*	9.03	1.39	1.39	*0.69*	1.39
14	10.42	8.33	9.72	*6.94*	10.42	8.33	*7.64*	*7.64*	*1.39*	*1.39*	*1.39*	2.08

Table 2. Error rates in %. Classes with 30 images filtered with Prewitt in case of Local Texture and GLCM Descriptors. Number of cycles is shown in rows and number of nodes in the hidden layer in columns.

	Local Texture				**GLCM Descriptors**				**Haralick Wavelet**			
	25	**100**	**200**	**1000**	**25**	**100**	**200**	**1000**	**25**	**100**	**200**	**1000**
2	*6.67*	7.5	7.5	*6.67*	*7.5*	8.75	*7.5*	*7.5*	*0.42*	*0.42*	0.83	1.67
4	13.33	*6.25*	7.08	7.92	*7.92*	10.83	10.42	8.75	*0.83*	*0.83*	6.67	2.08
6	9.17	7.5	7.08	*5.83*	10.83	10.83	*7.5*	8.33	1.25	0.42	0.42	***0.00***
8	8.33	*7.92*	17.08	*7.92*	10.42	*7.92*	9.17	9.58	0.83	*0.42*	6.67	2.08
10	7.5	*6.25*	7.5	10.83	8.33	*7.5*	16.67	8.75	1.25	*0.42*	*0.42*	2.08
14	5.83	7.08	*5*	5.42	10	9.58	*7.5*	9.17	0.83	2.92	0.42	***0.00***

Table 3. Error rates in %. Classes with 50 images filtered with Prewitt in case of Local Texture and GLCM Descriptors. Number of cycles is shown in rows and number of nodes in the hidden layer in columns.

Table 2 shows the global error rate for the case of thirty images in each class, used filtered images in Haralick descriptors, and non filtered images with the other two descriptors. Minimum error rate equals 0,69%. The values in the first row and first column are the number of cycles and the number of nodes in the hidden layer, respectively.

Table 3 and 4 show the global error rate for the other cases, that is, fifty and seventy images in each class. It is observed that the lower error rates correspond

	Local Texture				GLCM Descriptors				Haralick Wavelet			
	25	**100**	**200**	**1000**	**25**	**100**	**200**	**1000**	**25**	**100**	**200**	**1000**
2	11.31	11.01	10.12	*9.82*	*8.33*	8.63	8.93	10.42	*5.95*	8.04	9.52	9.23
4	16.96	*10.42*	16.37	11.9	10.42	*8.63*	9.52	9.52	***5.65***	7.44	7.74	6.55
6	*10.71*	11.01	*10.71*	12.2	*10.71*	16.96	11.31	*10.71*	*6.25*	7.44	6.85	7.14
8	10.12	11.01	10.71	*9.82*	10.71	11.31	13.69	*9.82*	7.44	8.04	*6.85*	7.14
10	*9.52*	16.07	11.01	13.69	12.2	12.8	*11.31*	*11.31*	9.82	*6.25*	7.74	7.74
14	16.07	12.5	15.77	*10.42*	*10.42*	10.71	12.5	12.5	7.74	*6.55*	*6.55*	7.44

Table 4. Error rates in %. Classes with 70 images filtered with Prewitt in case of Local Texture and GLCM Descriptors. Number of cycles is shown in rows and number of nodes in the hidden layer in columns.

to the fifty image case, even better than those obtained with thirty images. The best error rate obtained reaches the 0.0%.

The reason of this behavior may be that, in the case of thirty images, the training set is not large enough for optimum network learning and a reliable classification. In the case of seventy images the error rates increase up to 5,65% as expected, since values near to the decision border in both classes are very close, but even in this case, the Haralick descriptors achieve acceptable error rates.

4.3 Minimum Errors

Table 5 shows the minimum errors obtained with each descriptor and with both classification methods. The n parameter indicates that feature vectors are normalized. It can be observed that the MLP classifier gives better results in most of the cases, reaching its best result in the case of 50 images.

	30 images			50 images			70 images		
Class	**LText**	**GLCM**	**Har.W**	**LText**	**GLCM**	**Har.W**	**LText**	**GLCM**	**Har.W**
KNN	8.33	*6.65*	8.33	*5.00*	*5.00*	*5.00*	*7.86*	*7.86*	8.57
KNN n.	11.11	*6.11*	8.33	*4.00*	5.00	5.00	9.29	*6.90*	8.33
MLP	16.67	*1.39*	7.41	10.00	*3.33*	4.44	8.33	*7.14*	*7.14*
MLP n.	6.25	6.25	*0.69*	5.00	7.08	***0.00***	9.23	8.04	*5.65*

Table 5. Minimum errors with Local Texture Descriptors, Gray Level Co-ocurrence Matrix Descriptors and Haralick Descriptors.

5 Conclusions

This paper proposes a method based on computer vision to measure the surface finish quality of machined metallic parts. The performance of three different sets of descriptors was analyzed, applied on both filtered and unfiltered images. With k-nn classification filtered images showed a better performance, but with the neuronal network the non filtered images lead to lower error rates in the case of Haralick with wavelet descriptors.

The best results were achieved using neuronal network classification, with Haralick descriptors applied to the first subband of the wavelet transform and to the original image. This configuration leads to a classification accuracy of 100% when the first 50 and last 50 images were used. The results show that the use of texture descriptors is a feasible method to evaluate the roughness of metallic parts in the context of product quality and future research will focus on this line.

Acknowledgments. This work has been partially supported by the research projects DPI2006-02550 supported by the Spanish Ministry of Education and Science, ULE2005-01 by the University of León and LE018B06 by the Junta de Castilla y León.

References

1. Al-Kindi, G.A., Shirinzadeh, B. An evaluation of surface roughness parameters measurement using vision-based data. Intl. J. of Mach. Tools & Manuf., 47, 697-708 (2007)
2. Al-Kindi, G.A., Shirinzadeh, B. Feasibility assessment of vision-based surface roughness parameters acquisition for different types of machined specimens. Image and Vision Computing, 27, 444-458 (2009)
3. Al-Kindi, G.A.; Baul, R., Gill, K. An application of machine vision in the automated inspection of engineering surfaces. Intl. J. of Production Research, 30 (2), 241-253 (1992)
4. Castejón, M.; Alegre, E.; Barreiro, J., Hernández, L.K. On-line tool wear monitoring using geometric descriptors from digital images. Intl. J. of Machine Tools & Manufacture, 47, 1847-1853 (2007)
5. Gadelmawla, E. A vision system for surface roughness characterization using the gray level co-occurrence matrix. NDT& E Int., 37, 577-588 (2004)
6. ISO4288:1996. Geometrical product specification (GPS) Surface texture: Profile method
7. Kiran, M., Ramamoorthy, B., Radhakrishan, V. Evaluation of surface roughness by vision system. Intl. J. of Machine Tools and Manufacture, 38, 685-690 (1998)
8. Kumar, R., Kulashekar, P., Dhansekar, B., Ramamoorthy, B. Application of digital image magnification for surface roughness evaluation using machine vision. Intl. J. of Machine Tools and Manufacture, 45, 228-234 (2005)
9. Lee, B., Tarng, Y. Surface roughness inspection by computer vision in turning operations. Intl. J. of Machine Tools and Manufacture, 41, 1251-1263 (2001)
10. Lee, B., Hoa, S., Hob, S. Accurate estimation of surface roughness from texture features of the surface image using an adaptative neuro-fuzzy inference system. Precision Engineering, 29, 95-100 (2005)
11. Lee, B., Yu, S., Juan, H. The model of surface roughness inspection by vision system in turning. Mechatronics, 14 (1), 129-141 (2004)

12. Lee, B.; Juan, H., Yu, S. A study of computer vision for measuring surface roughness in the turning process. Intl. J. of Advanced Manufacturing Technology, 19, 295-301 (2002)
13. Lee, S., Chen, C. On-line surface roughness recognition system using artificial neural networks system in turning operations. The International Journal of Advanced Manufacturing Technology, 22 (7-8), 498-509 (2003)
14. Ramana, K., Ramamoorthy, B. Statistical methods to compare texture features of machined surfaces. Pattern Recognition, 29, 1447-1459 (1996)
15. Schmähling, F.A., Hamprecht, F.A., Hoffmann, D.M.P. A three-dimensional measure of surface roughness based on mathematical morphology. Intl. J. of Machine Tools and Manufacture, 46, 1764-1769 (2006)
16. Senin, N.; Ziliotti, M., Groppetti, R. Three-dimensional surface topography segmentation through clustering. Wear, 262, 395-410 (2007)
17. Tasan, Y., De Rooij, M. & Schipper, D. Measurement of wear on asperity level using image-processing techniques. Wear, 258, 83-91 (2005)
18. Tian, G.Y., Lu, R.S. & Gledhill, D. Surface measurement using active vision and light scattering. Optics and Lasers in Engineering, 45, 131-139 (2007)
19. Whitehouse, D.J. Handbook of surface and nanometrology. Institute of Physics Publishing (IOP) (2003)